

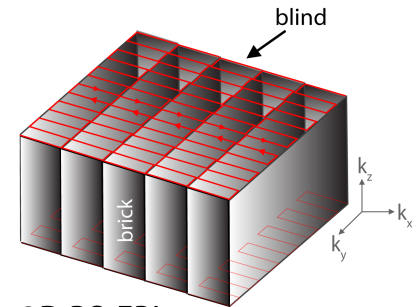
# Fast Susceptibility Weighted Imaging (SWI) using Readout-Segmented (RS)-EPI

S. J. Holdsworth<sup>1</sup>, R. O'Halloran<sup>1</sup>, S. Skare<sup>2</sup>, and R. Bammer<sup>1</sup>

<sup>1</sup>Department of Radiology, Stanford University, Palo Alto, CA, United States, <sup>2</sup>Clinical Neuroscience, Karolinska Institute, Stockholm, Sweden

**Introduction:** Susceptibility-weighted imaging (SWI) is an MRI technique that has been used to provide improved conspicuity of venous blood vessels and other sources of susceptibility effects [1,2]. The most commonly used SWI acquisition uses a 3D gradient echo (GRE) sequence, however due to the inefficient coverage of  $k$ -space per TR, 3D GRE suffers from a long scan time. In addition, even subtle motion in 3D GRE can considerably hamper the quality of final processed SWI image. A 3D EPI trajectory has been used as a faster alternative for SWI [3]. Unless 3D EPI is acquired with multiple interleaves (which consequently would also make it prone to motion artifacts), the images can suffer from significant blurring and geometric distortion. 3D Short-Axis Propeller (SAP)-EPI [4] has been proposed as a method to minimize distortion and blurring compared to 3D EPI for SWI, whilst keeping the scan time at a level appropriate for regular clinical use. A disadvantage of 3D SAP-EPI is the blurring that results from the combination of several EPI segments acquired at different angle. Readout-Segmented (RS)-EPI [5] is a similar technique to SAP-EPI, except that rather than acquiring several overlapping angular segments, adjacent overlapping segments are acquired. Since the segments are all acquired at the same angle, this results in reduced blurring in the final gridded image. Here we implement 3D RS-EPI as an alternative to 3D GRE and 3D SAP-EPI for SWI.

**Methods:** The 3D RS-EPI  $k$ -space trajectory is shown in Fig. 1. Experiments were conducted on a healthy volunteer using a 3T GE system and an 8-ch head coil. The following scan parameters were used: matrix size =  $288 \times 288$ , 7 blinds of width 64,  $R = 3$ , NEX = 3, TR/TE/FA = 55ms/20ms/15°, FOV =  $23 \times 23 \times 12.8\text{cm}^3$ , 64  $z$ -partitions, a 2 mm slice thickness, brick frame rate = 3.5s, and a scan time of 1:15min. For comparison a 3D SAP-EPI scan was acquired with equivalent scan parameters (1:15min scan time). A high resolution flow-compensated 3D GRE sequence was acquired for comparison using a matrix size =  $512 \times 256$ , rectangular FOV = 0.75, TR/TE/FA = 37ms/20ms/20°,  $z$ -partitions = 32, 2mm slice thickness, and a scan time = 4:40mins. All SWI images were produced by generating a phase mask using a 2D Hanning window for each individual coil, a multiplication of the phase mask by the magnitude coil by 5 times, followed by the sum of squares over coils. A minimum intensity projection (MinIP) was then taken over a 14mm thick stack of partitions.



**3D RS-EPI**

**Fig. 1:** 3D RS-EPI  $k$ -space trajectory. One segment (or blind) is acquired for every  $z$ -partition – resulting in one ‘brick’. Multiple adjacent overlapping bricks are acquired (overlap not shown for clarity).

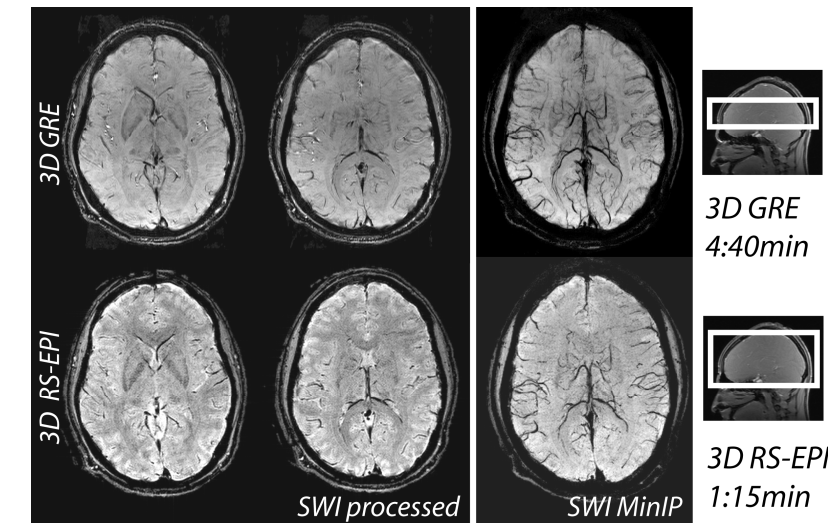


**Fig. 3:** Two slices from a 3D GRE and 3D RS-EPI sequence acquired with a matrix size of  $512 \times 256$  and  $288 \times 288$ , respectively, and a partition thickness of 2mm and a FOV of 23cm. A 14mm thick MinIP is also shown. As depicted schematically on the far right, 3D RS-EPI acquired full brain coverage (twice the coverage compared with 3D GRE) in a significantly reduced scan time.

processing. Due to the consistency of data within each brick, both 3D RS-EPI and 3D SAP-EPI image phase are significantly less sensitive to motion compared with both GRE and interleaved EPI. Furthermore, the small temporal footprint of the bricks (3.5s) for 3D RS-EPI makes it much easier than GRE to catch moderate motion and reacquire data if necessary. In addition, for jerky movement, as long as the brick frame rate in 3D RS-EPI is fast enough and there is enough overlap between bricks (to account for rotations of individual bricks), it may be possible to correct for motion between bricks in  $k$ -space in 3D. Future work will explore this claim. Further studies are warranted to perform a detailed comparative assessment of both 3D RS-EPI and 3D SAP-EPI methodologies to assess whether the (already demonstrated) motion-robust self-navigated 3D SAP-EPI is truly needed when the better resolved 3D RS-EPI can handle motion to an acceptable level as demonstrated in this study. Overall, the minimum gain in small vessel conspicuity of 3D GRE does not appear to justify the almost 4-fold longer scan time at half the coverage in cervico-caudal direction.

**References:** [1] Reichenbach JR. Radiology 1997;204:272-77. [2] Hacke EM. MRM 2004;52:612-18. [3] Patel MR. Stroke 1996;27:2321-2324. [4] Holdsworth SJ. ISMRM 2009; 756. [5] Porter D. ISMRM 2008;3262. **Acknowledgements:** NIH (5R01EB002711, 5R01EB008706, 3R01EB008706, 5R01EB006526, 5R21EB006860, 2P41RR009784), the Center of Advanced MR Technology at Stanford (P41RR09784), Lucas Foundation, Oak Foundation, and the Swedish Research Council (K2007-53P-20322-01-4).

**Results:** A comparison between the SWI images acquired with 3D GRE and 3D RS-EPI is shown in Fig. 2. Although the resolution and SNR is highest for the 3D GRE, the 3D RS-EPI images show that it is possible to acquire good quality SWI images with twice the brain coverage in about a third of the scan time. Fig. 3 shows a comparison between the SWI MinIPs for both 3D RS-EPI and 3D SAP-EPI acquired at the same target resolution and scan time. Because of the unidirectional distortion in 3D RS-EPI, it demonstrates better vessel conspicuity than 3D SAP-EPI.

**Discussion & Conclusion:** Here we have shown that 3D RS-EPI is a fast alternative technique to 3D GRE for SWI (Fig. 2). The acquisition of 3D RS-EPI SWI images in 1:15min makes this technique applicable for routine use in the clinics. Parallel imaging with  $R = 3$  was used in order to minimize distortion, whilst keeping each blind consistent (i.e. inter-blind motion is negligible). One can also reduce the scan time for 3D GRE for SWI through the use of parallel imaging, but our experiments have shown that this can come at a significant detriment to the SNR (data not shown). In addition, this study demonstrated superior resolution and conspicuity when using 3D RS-EPI over 3D SAP-EPI (Fig. 3).

Even subtle motion can be a major problem for standard SWI imaging, as it can corrupt the phase image used for the SWI

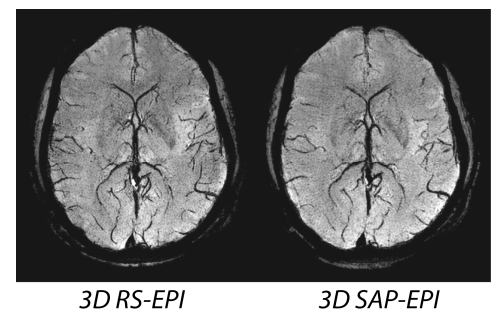


**Fig. 3:** (a) 3D RS-EPI, (b) 3D SAP-EPI SWI MinIP images acquired with the same scan time (1:15min). RS-EPI shows less blurring and better vessel conspicuity than SAP-EPI.